Uncertainty in projected changes in precipitation minus evaporation: dominant role of dynamic circulation changes and weak role for thermodynamic changes

Eilat Elbaum[1], Chaim I. Garfinkel[1], Ori Adam[1], Efrat Morin[1], Dorita Rostkier-Edelstein[1,2], Uri Dayan[3]

[1]Fredy and Nadine Herrmann Institute of Earth Sciences, Hebrew University, Jerusalem, Israel
[2]Department of Environmental Physics, Environmental Sciences Division, Israel Institute for Biological Research, Ness-Ziona, Israel.
[3]Department of Geography, Hebrew University, Jerusalem, Israel.

Key Points:

- Even in regions where thermodynamic changes drive the multi-model mean hydrologic changes, dynamic changes drive uncertainty.
- Dynamic changes more important for intermodel spread even after zonal averaging and even over subtropical oceans.
- Narrowing climate sensitivity will not help constrain future hydroclimate changes in most regions.

Corresponding author: Chaim I. Garfinkel, `chaim.garfinkel@mail.huji.ac.il`

Abstract

End of century projections from Coupled Model Intercomparison Project (CMIP) models show a decrease in precipitation over subtropical oceans that often extends into surrounding land areas, but with substantial intermodel spread. Changes in precipitation are controlled by both thermodynamical and dynamical processes, though the importance of these processes for regional scales and for intermodel spread is not well understood. The contribution of dynamic and thermodynamic processes to the model spread in regional precipitation minus evaporation (P-E) is computed for 48 CMIP models. The intermodel spread is dominated essentially everywhere by the change of the dynamic term, including in most regions where thermodynamic changes dominate the multi-model mean response. The dominant role of dynamic changes is insensitive to zonal averaging which removes any influence of stationary wave changes, and is also evident in subtropical oceanic regions. Relatedly, intermodel spread in P-E is generally unrelated to climate sensitivity.

Plain Language Summary

Climate change will lead to hydroclimate changes, however the physical process(es) whereby climate change leads to these hydroclimate change are still uncertain, especially on regional scales. The causes of intermodel spread, which determines the uncertainty in future projections, are also not well understood. We demonstrate that uncertainty in future changes are driven almost everwhere by changes in the large scale winds, while the precise amount of warming simulated by a given model is largely irrelevant. This highlights that reducing uncertainty in future hydroclimate changes requires primarily narrowing uncertainties in the circulation response.

1 Introduction

Earth's water cycle has already begun to change, and these changes will intensify as the climate warms (Manabe & Wetherald, 1980; Mitchell, 1983; Cubasch et al., 2001; Allen & Ingram, 2002), impacting societies and ecosystems throughout the world. The net water flux at the surface - precipitation minus evapotranspiration over land or precipitation minus evaporation over ocean (P - E) - is a key aspect of the water cycle as it regulates oceanic salinity and continental aridity. While globally averaged P - E must be zero both in the present climate and in the future, regional variability in P - E can arise from a range of dynamic and thermodynamic processes which are, in turn, affected by climate change.

Over oceans, projected changes in P - E on large scales appear to scale with changes in surface temperature in both the tropics (Chou & Neelin, 2004; Chou et al., 2009) and further poleward (Mitchell et al., 1987; Held & Soden, 2006; Byrne & O'Gorman, 2015). If future changes in relative humidity are assumed small, a simple thermodynamic scaling yields a change in P - E due to the Clausius-Clapeyron relation, with a moistening of the tropics and extratropics and a drying of the subtropics at a rate of approximately $7\%K^{-1}$ with respect to the local surface temperature change (Chou & Neelin, 2004; Held & Soden, 2006). This "wet-get-wetter, dry-get-drier" response is a consequence of increasing atmospheric water vapor content under a fixed wind pattern. On large spatial scales, this mechanism, along with its extensions to account for changes in temperature and relative humidity over land (Byrne & O'Gorman, 2015), appears to account for the multi-model mean response in many regions (Held & Soden, 2006; Byrne & O'Gorman, 2015; Polson & Hegerl, 2017). In addition to this thermodynamic mechanism, dynamic changes in winds contribute to precipitation changes, and can dominate the regional response in some regions (Chou et al., 2009; Scheff & Frierson, 2012; Huang et al., 2013; Zappa et al., 2015; Fereday et al., 2018; Mindlin et al., 2020; Zappa et al., 2020).

These thermodynamic and dynamic factors are important not just for the multi-model mean response, but also have been associated with intermodel variability in projected drying/wettening. Specifically, a larger increase in mean temperature due to a larger climate sensitivity in a given model would imply a stronger thermodynamic effect, while intermodel variability in circulation changes are associated with uncertainty in regional precipitation (Zappa et al., 2015; T. Shaw et al., 2016; Simpson et al., 2016, 2018; Garfinkel et al., 2020; Cao et al., 2020). An example of a region with a wide spread in model projections is the Eastern Mediterannean: CMIP models project a decrease of 20-30% of Mediterranean precipitation by the end of the 21st century as compared to present-day averages if the multi-model mean is computed (Giorgi & Lionello, 2008; Kelley et al., 2012; Polade et al., 2017; Tuel & Eltahir, 2020; Garfinkel et al., 2020). However, there is a wide spread among models participating in the fifth phase of CMIP (CMIP5), with projections ranging from essentially no change to over a 50% precipitation reduction (Zappa et al., 2015; Polade et al., 2017; Garfinkel et al., 2020). Spread in precipitation projections exists among models participating in the sixth phase of CMIP (CMIP6) as well, as demonstrated for different regions (Almazroui et al., 2020; Jiang et al., 2020; Monerie et al., 2020). As adaptation efforts will necessarily differ if the reduction is, say, 10% vs. 40%, a better understanding (and even narrowing) of the source of this spread is of crucial importance.

The goal of this work is to characterize the importance of dynamic vs. thermodynamic factors for the multi-model mean response and the intermodel spread in future P - E changes. After introducing the data and diagnostic tool in Section 2, we demonstrate that even in regions where multi-model mean changes in P - E are driven primarily by thermodynamic processes, intermodel spread both regionally and also upon taking zonal averages is driven by dynamical processes. This highlights that uncertainty in future hydro-climate changes both regionally and also on larger scales is driven in large part by poorly-constrained circulation changes.

2 Data and Methods

The comprehensive model simulations used here are taken from those submitted to the fifth and sixth phase of CMIP (CMIP5/6) (Taylor et al., 2012; Eyring et al., 2016). We focus on the high-emissions scenarios, RCP8.5 and SSP5-8.5, respectively. We consider 48 model simulations - 29 CMIP5 simulations and 19 CMIP6 simulations (Table 1). These models were selected according to the availability of the requisite data in the Earth System Grid Federation at the time this study was conducted. We consider the change between two 20-year periods, January 2015-December 2034 and January 2079-December 2098. Our analysis mainly focuses on the boreal extended winter half-year of November through April (NDJFMA), with results for May through October (MJJASO) in the supplemental material.

The contribution of thermodynamical and dynamical processes to P - E is diagnosed using the steady-state moisture budget in isobaric coordinates, using discrete model pressure levels (Seager, Liu, et al., 2014; Seager, Neelin, et al., 2014; Seager et al., 2019):

$$P - E = -\frac{1}{g\rho_w}\nabla \cdot \sum_{k=1}^{K} \mathbf{u}_k q_k dp_k \tag{1}$$

where P is precipitation, E is evapotranspiration, g is the gravity acceleration, ρ_w is the density of water, q is specific humidity, $\mathbf{u}$ is the vector horizontal velocity, k is the pressure level ranging from k=1 (surface) to K, and dp is the pressure thickness of each level. The variables in Eq. 1 can be separated into monthly means (overbars), departures from monthly means (primes - daily and sub-daily variations), and climatological monthly means (double overbars). Following Seager and Henderson (2013) and neglecting sub-monthly variations in dp_k, the climatological steady-state moisture budget can be written as:

$$\bar{\bar{P}} - \bar{\bar{E}} \approx -\frac{1}{g\rho_w}\left[\nabla \cdot \sum_{k=1}^{K} \overline{\bar{\mathbf{u}}_k \bar{q}_k \overline{dp_k}} + \nabla \cdot \sum_{k=1}^{K} \overline{\overline{\mathbf{u}'_k q'_k \overline{dp_k}}}\right]. \tag{2}$$

The first term on the right-hand side (RHS) of Eq. 2 is the moisture convergence by the mean flow, and the second term is the moisture convergence by transient eddies. In this study we focus on the mean flow term only, and leave for future work the contribution of transient eddies or surface processes to intermodel spread in the moisture budget. Note, however, that for all regions discussed in the results, more than 70% of the intermodel variance in P - E is linearly related to the monthly mean terms, and hence the neglected terms are relatively smaller. Next, we decompose the mean convergence into moisture advection and mass divergence terms,

$$\bar{\bar{P}} - \bar{\bar{E}} \approx -\frac{1}{g\rho_w}\left[\sum_{k=1}^{K} \overline{(\bar{\mathbf{u}}_k \cdot \nabla \bar{q}_k + \bar{q}_k \nabla \cdot \bar{\mathbf{u}}_k)\overline{dp_k}}\right]. \tag{3}$$

Denoting changes between the end-of-the-century (2079-2098) and the beginning-of-the-century (2015-2034) by Δ, Eq. 3 now becomes

$$\Delta(\bar{\bar{P}} - \bar{\bar{E}}) \approx -\frac{1}{g\rho_w}\sum_{k=1}^{K} \Delta\overline{(\bar{\mathbf{u}}_k \cdot \nabla \bar{q}_k)\overline{dp_k}} - \frac{1}{g\rho_w}\sum_{k=1}^{K} \Delta\overline{(\bar{q}_k \nabla \cdot \bar{\mathbf{u}}_k)\overline{dp_k}}. \tag{4}$$

Each of the two terms on the right-hand-side of Eq. 4 can be expanded out, and then rearranged as:

$$\Delta(\bar{\bar{P}} - \bar{\bar{E}}) \approx \Delta\text{thermodynamic} + \Delta\text{dynamic}, \tag{5}$$

where

$$\Delta\text{dynamic} = -\frac{1}{g\rho_w}\sum_{k=1}^{K} \Delta\overline{(\bar{\mathbf{u}}_k \overline{dp_k})} \cdot \nabla \bar{\bar{q}}_{k,botc} - \frac{1}{g\rho_w}\sum_{k=1}^{K} \bar{\bar{q}}_{k,botc}\Delta\overline{(\nabla \cdot \bar{\mathbf{u}}_k \overline{dp_k})} \tag{6}$$

and

$$\Delta\text{thermodynamic} = -\frac{1}{g\rho_w}\sum_{k=1}^{K} \bar{\bar{\mathbf{u}}}_{k,botc} \cdot \Delta\overline{(\nabla \bar{q}_k \overline{dp_k})} - \frac{1}{g\rho_w}\sum_{k=1}^{K} \nabla \cdot \bar{\bar{\mathbf{u}}}_{k,botc}\Delta\overline{(\bar{q}_k \overline{dp_k})} \tag{7}$$

where botc in a subscript denotes "beginning-of-the-century" values. Here, terms involving $\Delta\bar{\mathbf{u}}_k$ and $\bar{\bar{q}}_{k,botc}$ constitute the dynamic component of the mean change, while terms involving $\Delta\bar{q}_k$ and $\bar{\bar{\mathbf{u}}}_{k,botc}$ constitute the thermodynamic component. The second thermodynamic term is most closely identified with the "wet-get-wetter" argument, as it involves a fixed mass divergence field acting on an altered moisture field, but note that the thermodynamic term also includes an advection term of altered humidity gradients which is not necessarily small (Seager et al., 2019).

This decomposition of the mean flow moisture convergence is calculated for every month in each of the two study periods, and then averaged seasonally. All terms are computed using each model's spatial resolution, and then are interpolated to a common grid using linear interpolation. We use monthly data as these were available for more models than daily or sub-daily data and allowed for the inclusion of additional models. Future work should consider the role of the transient term in contributing to intermodel spread in projected (P - E) for regions in which the monthly mean terms do not account for most of the intermodel spread, though note that for all regions discussed in section

3 the monthly mean terms dominate and the residual is small. Statistical significance for correlation coefficients of the intermodel spread is computed using a two-tailed Student-t test at the 95% confidence level, and given 48 distinct models a correlation must exceed ± 0.29 for a p-value of 0.05. If the effective degrees of freedom is (arbitrarily) cut in half due to the fact that many models share code, the minimal correlation rises to ± 0.4. All results discussed in this paper exceed this higher ± 0.4 threshold too. One ensemble member is used for each model so as to not exclude modeling groups that only included one member but otherwise uploaded all data necessary to compute the (P - E) budget.

When considering factors leading to intermodel spread in Δ (P - E), we evaluate the linear correlation of Δ (P - E) with Δ thermodynamic and with Δ dynamic, with a higher positive correlation implying more explanatory power for the intermodel uncertainty in Δ (P - E). We also assess the extent to which model spread in Δ (P - E) is associated with model spread in changes over the same period of Δ globally averaged surface temperature (i.e. a measure of transient climate sensitivity), calculated as the difference in area-weighted global surface temperatures.

3 Results

The multi-model decomposition of changes to the moisture budget into a dynamic component and a thermodynamic component in NDJFMA is presented in Fig. 1. Fig. 1a and Fig. 1d show the multi-model mean changes in P - E in CMIP5 and CMIP6 respectively, and demonstrate that the overall projected changes in the two phases are similar. This similarity extends to the dynamic and thermodynamic terms (Equation 6 and 7) as well (Fig. 1bcef). In agreement with previous work, the dynamic term is dominant over the Mediterranean (Seager, Liu, et al., 2014) while the thermodynamic term dominates over the Pacific Northwest (Seager, Neelin, et al., 2014). The thermodynamic term dominates precipitation changes over tropical Africa, while the dynamic term is most important over the tropical Pacific, though in most of the rest of the tropics there is substantial cancellation as expected from energetic considerations (Chou & Neelin, 2004; Vecchi & Soden, 2007; Xie et al., 2010). Because of the similarity between CMIP5 and CMIP6 in Figure 1, similarities in dynamical changes discussed in Harvey et al. (2020) and Grise and Davis (2020), and also because CMIP5 and CMIP6 models are interspersed in subsequent figures in this paper showing intermodel scatter, we combine both generations in the rest of this paper. Zonally and annually averaged drying trends in the subtropics are driven primarily by the thermodynamic term (Supplemental Figure S1), in agreement with the dry-get-drier mechanism.

While both the dynamic and thermodynamic terms are important for multi-model mean changes, intermodel spread almost everywhere is dominated by the dynamic term. This is demonstrated in Figure 2, which shows the across-model correlation coefficient between $\Delta(\overline{P}-\overline{E})$ and the Δ dynamic (Figure 2a) and Δ thermodynamic (Figure 2b) terms. Over most oceanic and coastal regions, and also over many continental regions, intermodel spread in $\Delta(\overline{P}-\overline{E})$ is more closely related to intermodel spread in the Δ dynamic term. In contrast, there are only two regions where the spread in the Δ thermodynamic term is more important: the subtropical eastern margin of oceans (e.g. off the coast of West Africa, Namibia, and northern Chile), and also over the Sahara.

In many subtropical regions, including the Eastern Mediterranean over the Balkan Peninsula and over the Pacific north of Hawaii, the Δ thermodynamic term is negatively correlated with the simulated $\Delta(\overline{P}-\overline{E})$. In other words, a model with a particularly strong drying due to the thermodynamic term in these regions actually tends to simulate an overall wettening. We demonstrate this effect explicitly for the Balkan Peninsula (enclosed with a black square in Figure 2) in Figure 3ab. Figure 3 contrasts the $\Delta(\overline{P}-\overline{E})$ as simulated by each model with the Δ dynamic (Figure 3a) and Δ thermodynamic terms (Figure 3b) from each model. Consistent with previous work (Seager, Liu, et al., 2014), the multi-model mean change is driven by the dynamic term, and Figure 3a demonstrates that the intermodel spread is also driven by the dynamic term, with a statistically significant correlation coefficient of 0.83. The thermodynamic term acts as if it were a negative feedback (correlation coefficient of -0.6): models with a stronger decrease in $(\overline{P} - \overline{E})$ tend to also simulate a moistening from the thermodynamic term.

Even in regions where the multi-model mean change in $\Delta(\overline{P} - \overline{E})$ is dominated by the Δ thermodynamic term, the Δ dynamic term is in most cases more important for intermodel spread. An example of such a region is the Pacific Northwest (enclosed with a blue square in Figure 2), and we show the changes in each model for this region in Figure 3cd. The Δ thermodynamic term leads to projected moistening in almost all models, however the magnitude of Δ thermodynamic in a given model is generally unrelated to the actual change in $\Delta(\overline{P}-\overline{E})$ simulated by that model (Figure 3d). In contrast, the intermodel spread in the Δ dynamic term determines the intermodel spread in $\Delta(\overline{P}-\overline{E})$, and this intermodel spread is several times larger in amplitude than the multi-model mean Δ thermodynamic change. The net effect is that uncertainty in the circulation response to global warming dominates future uncertainty in the hydrologic cycle especially at regional scales.

Thermodynamic effects play a particularly large role for multi-model mean future drying in the subtropical oceans (Fig. 1), and we now focus on whether thermodynamic effects play a role in inter-model spread in such a region in Figure 3ef. Specifically, Figure 3ef compares the actual $\Delta(\overline{P}-\overline{E})$ in the subtropical North Pacific ocean (enclosed with a magenta square in Figure 2) simulated by each model to its Δ dynamic (Figure 3e) and Δ thermodynamic components (Figure 3f) in the annual average. Note that the chosen region is broader than the regions selected for Figure 3a-d. The intermodel spread in subtropical Pacific drying is dictated entirely by the Δ dynamic term (Figure 3e). In contrast, the Δ thermodynamic term is negatively correlated with the actual $\Delta(\overline{P}-\overline{E})$ (Figure 3f; similar to the Balkan region discussed in Figure 3ab), with models simulating a greater thermodynamic drying also simulating an overall wettening. Hence, averaging over a broad region, or over a subtropical oceanic region, does not necessarily lead to a larger role for the thermodynamic term in explaining intermodel spread.

For two of the regions considered in Figure 3, the sign of the correlation of intermodel spread with the Δ dynamic term was opposite that of the Δ thermodynamic term. Note that changes in the dynamic and thermodynamic components generally tend to balance each other in the multi-model mean as well (Figure 1). While the mechanism for compensation likely differs regionally, one example of such a mechanism is the "ventilation effect" (Su & Neelin, 2005) where increased land-sea contrasts drive stronger circulation which increases precipitation, but reduce relative humidity, which decreases precipitation. It is therefore not a trivial result that thermodynamic changes contribute so little to model spread in Figure 2 in most other regions.

Thus far we have focused on regional changes in the hydrologic cycle, and perhaps it is not surprising that for regional changes intermodel uncertainty is driven by circulation uncertainty, as changes in stationary waves (Wills et al., 2019) are known to influence regional hydroclimate (Wills & Schneider, 2016; Simpson et al., 2016). In order to minimize the effect of such stationary wave changes on the dynamic term, we now focus on the role of the thermodynamic and dynamic terms for intermodel spread in $\Delta(\overline{P}-\overline{E})$ after zonal and meridional averaging.

Figure 4ab shows the correlation of zonally averaged $\Delta(\overline{P}-\overline{E})$ with the zonally averaged Δ thermodynamic and Δ dynamic terms. For most latitude bands and both in NDJFMA and MJJASO, spread in zonally averaged $\Delta(\overline{P}-\overline{E})$ is dominated by intermodel spread in the Δ dynamic term. The only exceptions are the poleward edges of the subtropics in the winter hemisphere, where the dynamic and thermodynamic terms have a roughly equal contribution to intermodel spread in $\Delta(\overline{P} - \overline{E})$.

The relative dominance of dynamic changes for intermodel spread in $\Delta(\overline{P} - \overline{E})$ is also evident if we additionally perform a limited meridional average. Specifically, we average each of $\Delta(\overline{P}-\overline{E})$, Δ dynamic, and Δ thermodynamic both zonally and meridionally within a running 10° window (5° to the north and south at each latitude), and then compute the correlations (Figure 4cd). Results are generally a smoothed version of Figure 4ab, with the Δ thermodynamic term only comparable to the Δ dynamical term in the subtropical winter hemisphere and between 50° and 60° in the extratropics. Only if a 20° averaging window (10° north and south) is adopted are the thermodynamic and dynamic terms roughly of equal importance for intermodel spread in midlatitude $\Delta(\overline{P}-\overline{E})$ (not shown), and for an averaging window of 30° meridionally the Δ dynamic term is no longer important for intermodel spread in midlatitude $\Delta(\overline{P} - \overline{E})$. Such a result is perhaps expected from Fig. 1, as the dynamic changes are relatively more confined to specific latitude bands.

Thus far we have demonstrated that the thermodynamic term is generally unimportant for the uncertainty in hydroclimate changes with only limited exceptions. At first glance this result may be surprising, as the thermodynamic term has been linked to the overall globally averaged warming, and hence we now explore this result. First, we confirm that the spread in Δ thermodynamic is strongly related to the spread in projected warming among the models. Figure 2c shows the correlation of the intermodel spread of the change in near-surface globally averaged temperature (ΔT_{global}) with the Δ thermodynamic term at each grid point. Correlations are generally positive in the tropics and negative in the subtropics, which implies a model with more warming will experience a stronger wettening in the tropics and more drying in the subtropics. That is, we confirm that in a model with more warming, the "wet-get-wetter" thermodynamic effect is even more pronounced, as predicted by the Clausius-Clapeyron equation.

However this thermodynamic effect is largely irrelevant for the overall intermodel spread in $\Delta(\overline{P}-\overline{E})$. We demonstrate this in Figure 2d, which shows the correlation of the intermodel spread of the change in globally averaged temperature (ΔT_{global}) with intermodel spread in $\Delta(\overline{P} - \overline{E})$. The patterns in Figure 2c and Figure 2d differ (pattern correlation of 0.16). The patterns are similar only over Africa, the Middle East, and the North Atlantic, but over other regions are in general opposite, implying that any contribution from the thermodynamic term is overwhelmed by other processes. Hence, transient climate sensitivity is indeed important for thermodynamic changes (consistent with Clausius-Clapeyron), but not for the inter-model uncertainty in net regional hydroclimate changes.

This effect is shown explicitly for the subtropical North Pacific in Figure 3gh. Figure 3g contrasts ΔT_{global} with the Δ dynamic term in each model, and Figure 3h is similar but for the Δ thermodynamic term. The change in the thermodynamic term is highly correlated with the globally-averaged warming (correlation of -0.73), with a model exhibiting more warming also simulating more drying via the thermodynamic term. In contrast, intermodel spread in the Δ dynamic term and globally-averaged warming are only weakly related (Figure 3g). However, for this region, the Δ thermodynamic term is anticorrelated with intermodel spread of $\Delta(\overline{P}-\overline{E})$ (Figure 3f), and consistent with this the relationship between intermodel spread in ΔT_{global} and $\Delta(\overline{P}-\overline{E})$ is opposite what one would expect if the thermodynamic term dominated. Namely, if the thermodynamic term dominated then models simulating more warming should also simulate a more negative $\Delta(\overline{P}-\overline{E})$, but in reality, the opposite occurs: models simulating a large ΔT_{global} simulate a positive $\Delta(\overline{P} - \overline{E})$ (magenta square on Figure 2d).

Results are generally similar for the Southern Hemisphere winter season. Drying over the subtropical Indian and Atlantic Oceans is mostly from the thermodynamic term, and this drying extends over Southern Africa and Central Chile from 35S to 45S (Supplemental Figure S2). However intermodel uncertainty in most regions in Δ (P - E) is driven by the Δ dynamic term (Supplemental Figure S3), with central Chile the main exception over land. The net effect is that even though multi-model mean drying over South Africa is driven by the Δ thermodynamic term (Supplemental Figure S4b), the across model spread is driven by the Δ dynamic term (Supplemental Figure S4a).

4 Discussion

A relatively robust projection from CMIP models is that the poleward edge of the subtropics in most regions will dry in response to climate change, however the magnitude of this projected change varies among the models from essentially no change to a 50% reduction in some regions (Zappa et al., 2015; Polade et al., 2017; Garfinkel et al., 2020). As the scope of adaptation efforts will depend on the magnitude of the drying, it is important to understand the causes of this spread, with the hope of potentially narrowing it.

One of the simplest mechanisms that aims to explain this subtropical drying is a thermodynamic effect: the dry get dryer and wet get wetter due to Clausius Clapeyron scaling (Held & Soden, 2006). We demonstrated in this paper that while this thermodynamic effect may be important for the multi-model mean response, it is overwhelmed by other sources of uncertainty and thus rendered irrelevant for understanding the intermodel spread. This irrelevance is not just due to dynamical stationary wave changes, as even if we zonally average, the uncertainty from dynamical processes is still dominant in most latitude bands. This irrelevance also extends to the subtropical oceans, which are perhaps the clearest example of dry-get-dryer when considering the multi-model mean. Rather, dynamical processes govern future hydroclimate uncertainty almost everywhere (the only notable exceptions are the eastern margin of the subtropical oceans).

There are many dynamical mechanisms that could lead to a drying on the equatorward flank of currently wet midlatitude regions (T. A. Shaw, 2019), and future work should consider whether these mechanisms are represented differently among models and hence may shed light on the causes of intermodel differences in future drying. Relatedly, dynamical changes can be driven as the residual of a tug-of-war of many competing thermodynamic starting points (e.g., large-scale changes in Arctic amplification or tropical upper tropospheric warming; T. Shaw et al., 2016), and while changes in each thermodynamic starting point are robust and well-understood (Shepherd, 2014; Vallis et al., 2015; T. A. Shaw, 2019), the magnitude of projected net changes are uncertain, though this uncertainty can be utilized to offer a storyline of possible dynamical changes (Zappa & Shepherd, 2017; Zappa, 2019; Mindlin et al., 2020; Garfinkel et al., 2020). Furthermore, stationary wave changes can influence the regional hydroclimate (Simpson et al., 2016; Tuel & Eltahir, 2020), and using the framework of Section 2 this effect occurs through the dynamic term. In addition to such (potentially reducible) model structural differences in dynamical changes, models also may differ in the dynamic term due to internal variability (i.e. unforced changes in the climate state; Deser et al., 2012). The dynamical changes identified here include both these model structural differences and internal variability, and only by considering large ensembles (e.g. McKenna & Maycock, 2021) can these possibilities be distinguished. However the limited number of modeling centers producing such large ensembles likely limits the conclusions that could be reached concerning whether model structural differences may lead to differences in projected drying.

Regardless of the source of this intermodel uncertainty in dynamics, narrowing this dynamical uncertainty is crucial for future adaptation given its importance for uncertainty in future hydroclimate. In contrast, narrowing climate sensitivity will not help narrow uncertainty in future hydroclimate in most regions. This implies that it is more important for regional downscaling excercises, e.g., CORDEX to sample models with a wide range of circulation responses to climate change, while it is relatively less critical to sample models with a wide range of climate sensitivities.

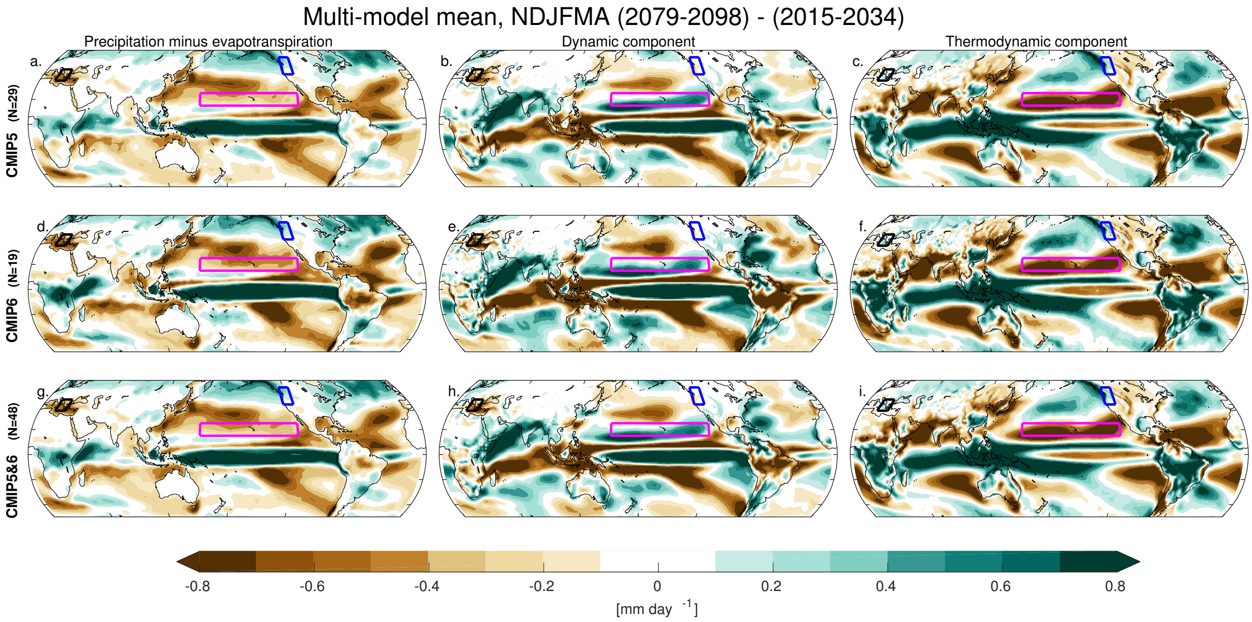

Figure 1. CMIP5 multi-model mean of average NDJFMA changes in (a) precipitation minus evapotranspiration, (b) dynamic component, and (c) thermodynamic component. (d-f) Same as (a-c) for CMIP6 multi-model mean, (g-i) same as (a-c) for CMIP5 and CMIP6 combined multi-model mean. Boxes show the boundaries of the Mediterranean region, Pacific Northwest region and subtropical Pacific region for Figure 3. The contours and colorbars are chosen to emphasize midlatitude changes.

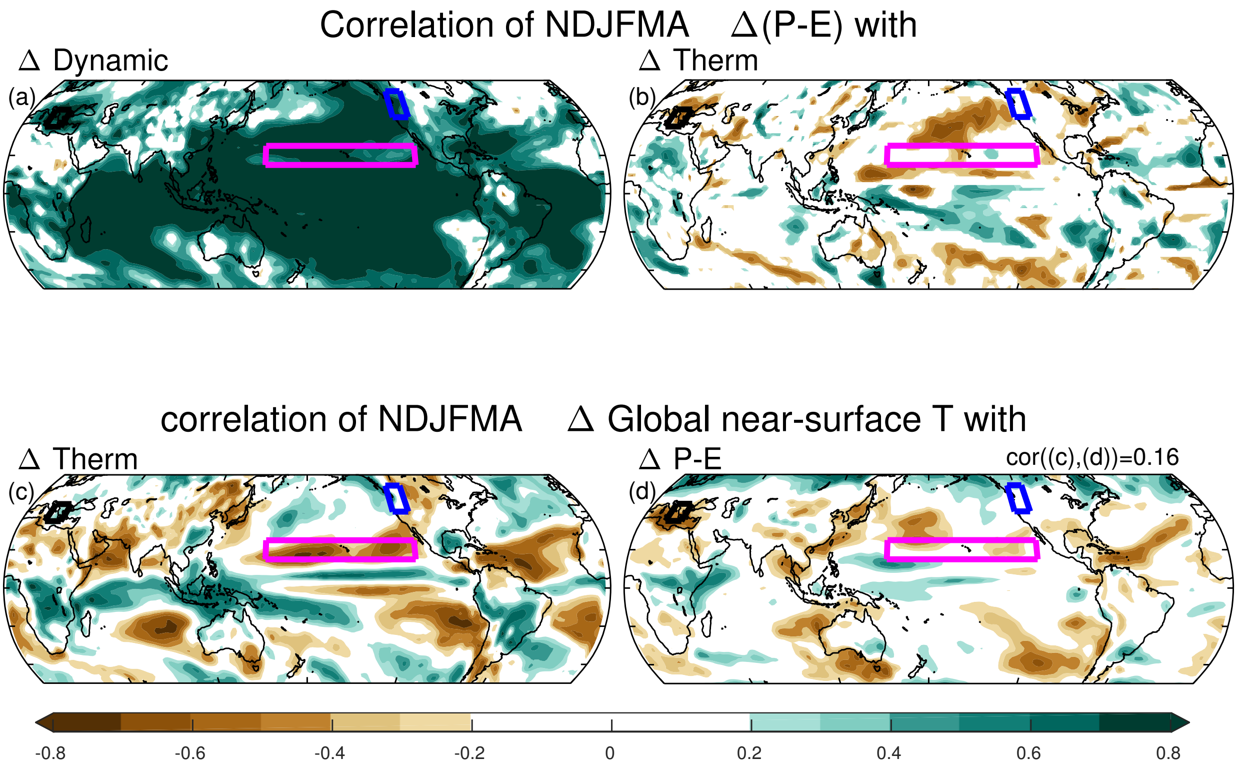

Figure 2. (top) Correlation coefficients across all 48 models of the NDJFMA change in precipitation minus evapotranspiration with the NDJFMA change in the (a) dynamic component and (b) thermodynamic component. (bottom) Correlation of the change in ΔT_{global} with the change in the (c) thermodynamic term and (d) P - E for each gridpoint. Boxes show the boundaries of the Mediterranean region, Pacific Northwest region, and subtropical Pacific region for Figure 3. Correlation coefficients exceeding ±0.29 can lead to the rejection of a null hypothesis of no relationship at the 95% confidence level using a two-tailed Student-t test given 48 distinct models.

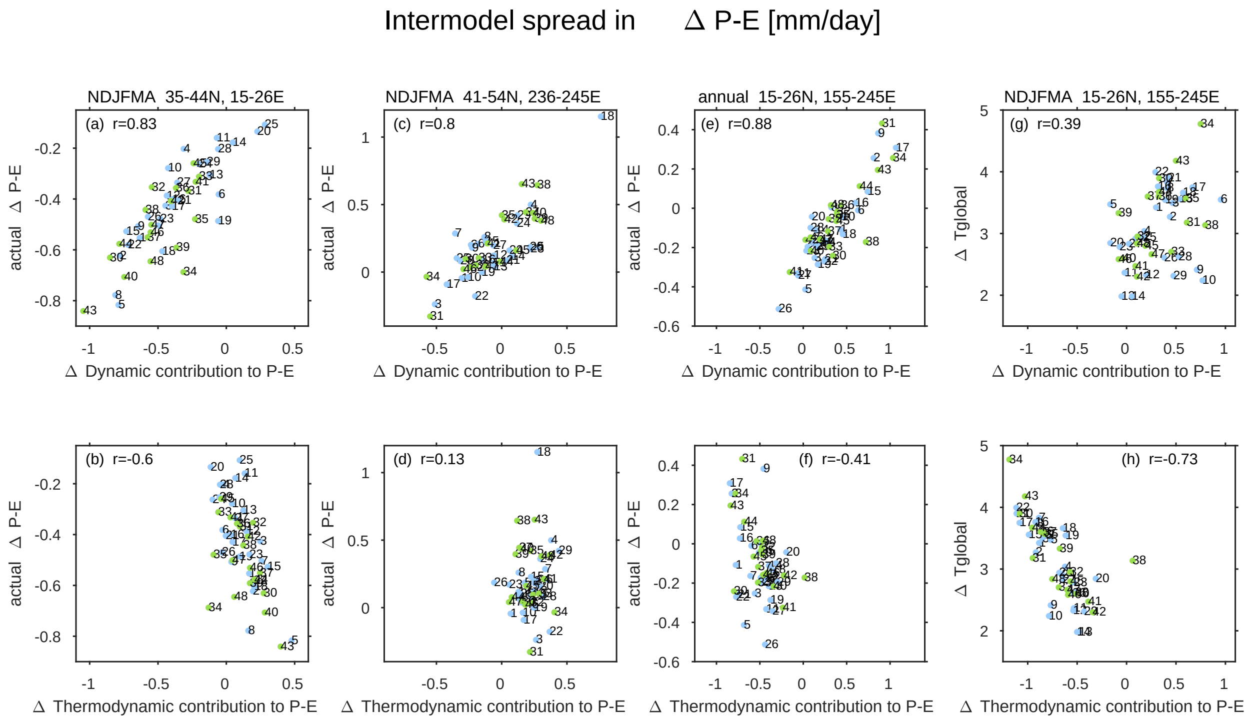

Figure 3. The change in $(\overline{P} - \overline{E})$ actually simulated by each model as compared to the change in the dynamic and thermodynamic terms for (ab) the Balkan Peninsula region (enclosed with a black square in Figure 2); (cd) the Pacific Northwest (enclosed with a blue square in Figure 2); (ef) the subtropical Pacific Ocean (enclosed with a magenta square in Figure 2). (gh) The change in T_{global} simulated by each model as compared to the Δ dynamic and thermodynamic terms for the subtropical Pacific Ocean (enclosed with a magenta square in Figure 2). Correlation coefficients exceeding ± 0.29 (± 0.40) can lead to the rejection of a null hypothesis of no relationship at the 95% confidence level using a two-tailed Student-t test given 48 (24) distinct models. Numbering of models follows Table 1, with CMIP6 models in green and CMIP5 models in blue.

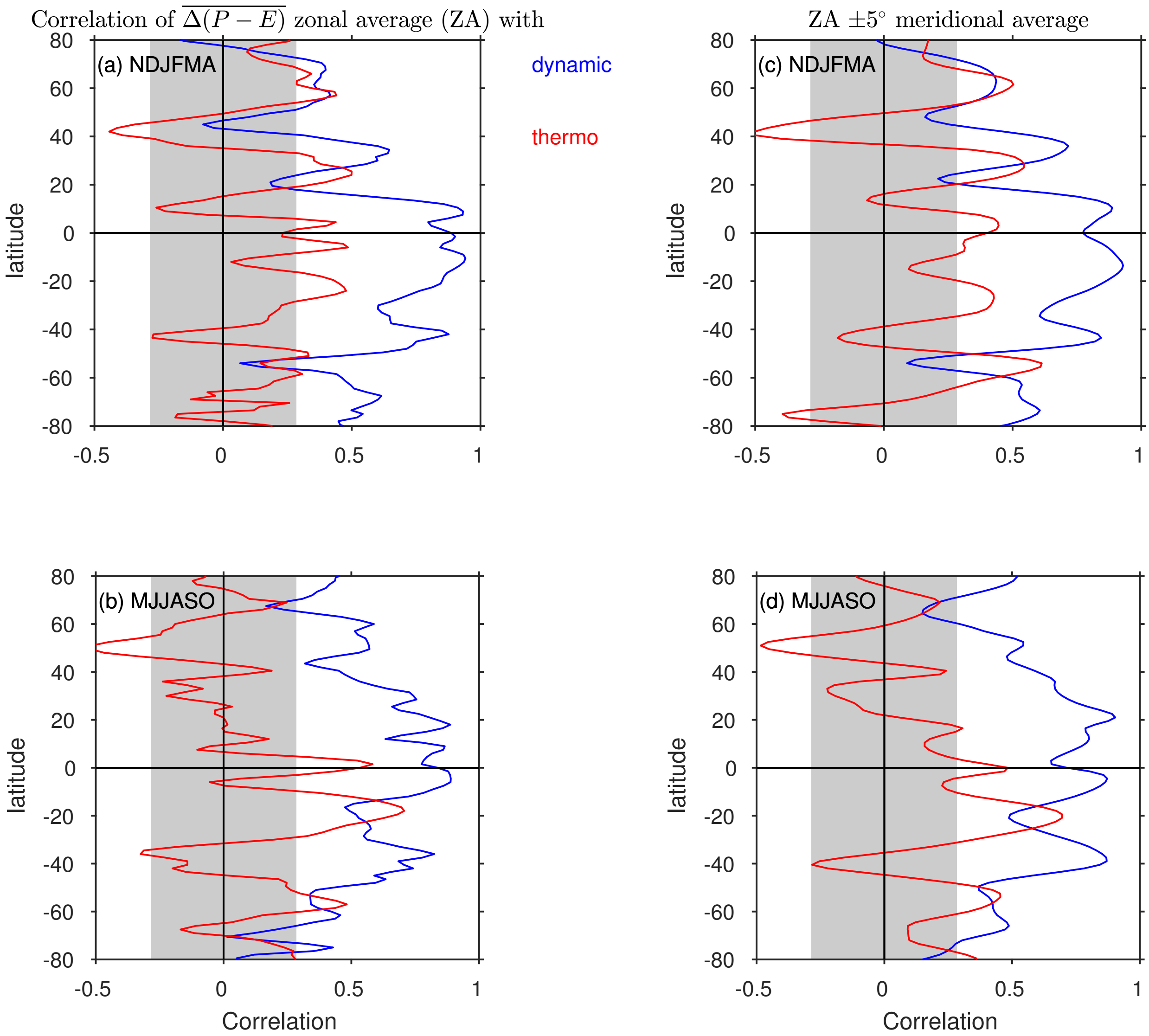

Figure 4. Correlation coefficients across all 48 models of the (top) NDJFMA and (bottom) MJJASO change in precipitation minus evapotranspiration with (blue) Δ dynamic component and (red) Δ thermodynamic components, after (left) first performing a zonal average, and (right) first performing a zonal average and a meridional averaging over a window of 10°. Gray shading indicates a correlation not statistically significant at the 95% level using a two-tailed Students-t test.

Table 1. CMIP5 models (1-29) and CMIP6 models (30-48) used in this study

1	ACCESS1-0	2	ACCESS1-3	3	BNU-ESM
4	CNRM-CM5	5	CSIRO-Mk3-6-0	6	CanESM2
7	FGOALS-s2	8	GFDL-CM3	9	GFDL-ESM2G
10	GFDL-ESM2M	11	GISS-E2-H	12	GISS-E2-H-CC
13	GISS-E2-R	14	GISS-E2-R-CC	15	HadGEM2-AO
16	HadGEM2-CC	17	HadGEM2-ES	18	IPSL-CM5A-LR
19	IPSL-CM5A-MR	20	IPSL-CM5B-LR	21	MIROC-ESM
22	MIROC-ESM-CHEM	23	MIROC5	24	MRI-CGCM3
25	MRI-ESM1	26	NorESM1-M	27	bcc-csm1-1
28	bcc-csm1-1-m	29	inmcm4	30	ACCESS-CM2
31	ACCESS-ESM1-5	32	AWI-CM-1-1-MR	33	BCC-CSM2-MR
34	CanESM5	35	CMCC-CM2-SR5	36	EC-Earth3
37	EC-Earth3-Veg	38	FGOALS-f3-L	39	GFDL-CM4
40	GFDL-ESM4	41	INM-CM4-8	42	INM-CM5-0
43	IPSL-CM6A-LR	44	KACE-1-0-G	45	MIROC6
46	MPI-ESM1-2-HR	47	MPI-ESM1-2-LR	48	MRI-ESM2-0

5 Open Research

Data is freely available for download from the Earth System Grid Federation (ESGF) `https://esgf-node.llnl.gov/projects/cmip6/`.

Acknowledgments

This work is supported by the Israel Ministry of Science (grant number 61792). CIG was also supported by the Isreal Science Foundation grant 1727/21. We acknowledge the World Climate Research Programme, which, through its Working Group on Coupled Modeling, coordinated and promoted CMIP5/6. We thank the climate modeling groups for producing and making available their model output; the Earth System Grid Federation (ESGF) for archiving the data and providing access; and the multiple funding agencies who support CMIP5/6 and ESGF.

References

Allen, M. R., & Ingram, W. J. (2002). Constraints on future changes in climate and the hydrologic cycle. *Nature*, *419*(6903), 224.

Almazroui, M., Saeed, S., Saeed, F., Islam, M. N., & Ismail, M. (2020). Projections of precipitation and temperature over the south asian countries in cmip6. *Earth Systems and Environment*, *4*(2), 297–320.

Byrne, M. P., & O'Gorman, P. A. (2015). The response of precipitation minus evapotranspiration to climate warming: Why the wet-get-wetter, dry-get-drier scaling does not hold over land. *Journal of Climate*, *28*(20), 8078 - 8092. Retrieved from `https://journals.ametsoc.org/view/journals/clim/28/20/jcli-d-15-0369.1.xml` doi: 10.1175/JCLI-D-15-0369.1

Cao, J., Wang, B., Wang, B., Zhao, H., Wang, C., & Han, Y. (2020). Sources of the intermodel spread in projected global monsoon hydrological sensitivity. *Geophysical Research Letters*, *47*(18), e2020GL089560.

Chou, C., & Neelin, J. D. (2004). Mechanisms of global warming impacts on regional tropical precipitation. *Journal of climate*, *17*(13), 2688–2701.

Chou, C., Neelin, J. D., Chen, C.-A., & Tu, J.-Y. (2009). Evaluating the rich-get-richer mechanism in tropical precipitation change under global warming. *Journal of climate*, *22*(8), 1982–2005.

Cubasch, U., Meehl, G., Boer, G., Stouffer, R., Dix, M., Noda, A., ... others (2001). Projections of future climate change. climate change 2001: the scientific basis. contribution of working group i to the third assessment report of the intergovernmental panel on climate change. *J. T. Houghton et al., Eds., (New York: Cambridge University. Press)*, 526–582.

Deser, C., Phillips, A., Bourdette, V., & Teng, H. (2012). Uncertainty in climate change projections: the role of internal variability. *Climate dynamics*, *38*(3), 527–546.

Eyring, V., Bony, S., Meehl, G. A., Senior, C. A., Stevens, B., Stouffer, R. J., & Taylor, K. E. (2016). Overview of the coupled model intercomparison project phase 6 (cmip6) experimental design and organization. *Geoscientific Model Development*, *9*(5), 1937–1958.

Fereday, D., Chadwick, R., Knight, J., & Scaife, A. A. (2018). Atmospheric dynamics is the largest source of uncertainty in future winter european rainfall. *Journal of Climate*, *31*(3), 963–977.

Garfinkel, C. I., Adam, O., Morin, E., Enzel, Y., Elbaum, E., Bartov, M., ... Dayan, U. (2020). The role of zonally averaged climate change in contributing to intermodel spread in cmip5 predicted local precipitation changes. *Journal of Climate*, *33*(3), 1141–1154.

Giorgi, F., & Lionello, P. (2008). Climate change projections for the mediterranean region. *Global and planetary change*, *63*(2-3), 90–104.

Grise, K. M., & Davis, S. M. (2020). Hadley cell expansion in cmip6 models. *Atmospheric Chemistry and Physics*, *20*(9), 5249–5268.

Harvey, B., Cook, P., Shaffrey, L., & Schiemann, R. (2020). The response of the northern hemisphere storm tracks and jet streams to climate change in the cmip3, cmip5, and cmip6 climate models. *Journal of Geophysical Research: Atmospheres*, *125*(23), e2020JD032701.

Held, I. M., & Soden, B. J. (2006). Robust responses of the hydrological cycle to global warming. *Journal of climate*, *19*(21), 5686–5699.

Huang, P., Xie, S.-P., Hu, K., Huang, G., & Huang, R. (2013). Patterns of the seasonal response of tropical rainfall to global warming. *Nature Geoscience*, *6*(5), 357–361.

Jiang, J., Zhou, T., Chen, X., & Zhang, L. (2020). Future changes in precipitation over central asia based on cmip6 projections. *Environmental Research Letters*, *15*(5), 054009.

Kelley, C., Ting, M., Seager, R., & Kushnir, Y. (2012). Mediterranean precipitation climatology, seasonal cycle, and trend as simulated by cmip5. *Geophysical Research Letters*, *39*(21).

Manabe, S., & Wetherald, R. T. (1980). On the distribution of climate change resulting from an increase in co2 content of the atmosphere. *Journal of the Atmospheric Sciences*, *37*(1), 99-118. doi: 10.1175/1520-0469(1980)037⟨0099:OTDOCC⟩2.0.CO;2

McKenna, C. M., & Maycock, A. C. (2021). Sources of uncertainty in multimodel large ensemble projections of the winter north atlantic oscillation. *Geophysical Research Letters*, *48*(14), e2021GL093258. Retrieved from `https://agupubs.onlinelibrary.wiley.com/doi/abs/10.1029/2021GL093258` (e2021GL093258 2021GL093258) doi: https://doi.org/10.1029/2021GL093258

Mindlin, J., Shepherd, T. G., Vera, C. S., Osman, M., Zappa, G., Lee, R. W., & Hodges, K. I. (2020). Storyline description of southern hemisphere midlatitude circulation and precipitation response to greenhouse gas forcing. *Climate Dynamics*, *54*(9), 4399–4421.

Mitchell, J. F. (1983). The seasonal response of a general circulation model to changes in co2 and sea temperatures. *Quarterly Journal of the Royal Meteorological Society*, *109*(459), 113–152.

Mitchell, J. F., Wilson, C., & Cunnington, W. (1987). On co2 climate sensitivity and model dependence of results. *Quarterly Journal of the Royal Meteorological Society*, *113*(475), 293–322.

Monerie, P.-A., Wainwright, C. M., Sidibe, M., & Akinsanola, A. A. (2020). Model uncertainties in climate change impacts on sahel precipitation in ensembles of cmip5 and cmip6 simulations. *Climate Dynamics*, *55*(5), 1385–1401.

Polade, S. D., Gershunov, A., Cayan, D. R., Dettinger, M. D., & Pierce, D. W. (2017). Precipitation in a warming world: Assessing projected hydro-climate changes in california and other mediterranean climate regions. *Scientific reports*, *7*(1), 1–10.

Polson, D., & Hegerl, G. C. (2017). Strengthening contrast between precipitation in tropical wet and dry regions. *Geophysical Research Letters*, *44*(1), 365-373. Retrieved from `https://agupubs.onlinelibrary.wiley.com/doi/abs/10.1002/2016GL071194` doi: https://doi.org/10.1002/2016GL071194

Scheff, J., & Frierson, D. (2012). Twenty-first-century multimodel subtropical precipitation declines are mostly midlatitude shifts. *Journal of Climate*, *25*(12), 4330–4347.

Seager, R., & Henderson, N. (2013). Diagnostic computation of moisture budgets in the era-interim reanalysis with reference to analysis of cmip-archived atmospheric model data. *Journal of Climate*, *26*(20), 7876–7901.

Seager, R., Liu, H., Henderson, N., Simpson, I., Kelley, C., Shaw, T., . . . Ting, M. (2014). Causes of increasing aridification of the mediterranean region in response to rising greenhouse gases. *Journal of Climate*, *27*(12), 4655–4676.

Seager, R., Neelin, D., Simpson, I., Liu, H., Henderson, N., Shaw, T., . . . Cook, B. (2014). Dynamical and thermodynamical causes of large-scale changes in the hydrological cycle over north america in response to global warming. *Journal of Climate*, *27*(20), 7921 - 7948. Retrieved from `https://journals.ametsoc.org/view/journals/clim/27/20/jcli-d-14-00153.1.xml` doi: 10.1175/JCLI-D-14-00153.1

Seager, R., Osborn, T. J., Kushnir, Y., Simpson, I. R., Nakamura, J., & Liu, H. (2019). Climate variability and change of mediterranean-type climates. *Journal of Climate*, *32*(10), 2887 - 2915. Retrieved from `https://journals.ametsoc.org/view/journals/clim/32/10/jcli-d-18-0472.1.xml` doi: 10.1175/JCLI-D-18-0472.1

Shaw, T., Baldwin, M., Barnes, E. A., Caballero, R., Garfinkel, C., Hwang, Y.-T., . . . others (2016). Storm track processes and the opposing influences of climate change. *Nature Geoscience*, *9*(9), 656–664.

Shaw, T. A. (2019). Mechanisms of future predicted changes in the zonal mean midlatitude circulation. *Current Climate Change Reports*, *5*(4), 345–357.

Shepherd, T. G. (2014). Atmospheric circulation as a source of uncertainty in climate change projections. *Nature Geoscience*, *7*(10), 703.

Simpson, I. R., Hitchcock, P., Seager, R., Wu, Y., & Callaghan, P. (2018). The downward influence of uncertainty in the northern hemisphere stratospheric polar vortex response to climate change. *Journal of Climate*, *31*(16), 6371–6391.

Simpson, I. R., Seager, R., Ting, M., & Shaw, T. A. (2016). Causes of change in northern hemisphere winter meridional winds and regional hydroclimate. *Nature Climate Change*, *6*(1), 65.

Su, H., & Neelin, J. D. (2005). Dynamical mechanisms for african monsoon changes during the mid-holocene. *Journal of Geophysical Research: Atmospheres*, *110*(D19). Retrieved from `https://agupubs.onlinelibrary.wiley.com/doi/abs/10.1029/2005JD005806` doi: https://doi.org/10.1029/2005JD005806

Taylor, K. E., Stouffer, R. J., & Meehl, G. A. (2012). An overview of cmip5 and the experiment design. *Bulletin of the American Meteorological Society*, *93*(4), 485–498.

Tuel, A., & Eltahir, E. A. (2020). Why is the mediterranean a climate change hot spot? *Journal of Climate*, *33*(14), 5829–5843.

Vallis, G. K., Zurita-Gotor, P., Cairns, C., & Kidston, J. (2015). Response of the large-scale structure of the atmosphere to global warming. *Quarterly Journal of the Royal Meteorological Society*, *141*(690), 1479–1501.

Vecchi, G. A., & Soden, B. J. (2007). Global warming and the weakening of the tropical circulation. *Journal of Climate*, *20*(17), 4316–4340.

Wills, R. C., & Schneider, T. (2016). How stationary eddies shape changes in the hydrological cycle: Zonally asymmetric experiments in an idealized gcm. *Journal of Climate*, *29*(9), 3161–3179.

Wills, R. C., White, R. H., & Levine, X. J. (2019). Northern hemisphere stationary waves in a changing climate. *Current climate change reports*, *5*(4), 372–389.

Xie, S.-P., Deser, C., Vecchi, G. A., Ma, J., Teng, H., & Wittenberg, A. T. (2010). Global warming pattern formation: Sea surface temperature and rainfall. *Journal of Climate*, *23*(4), 966–986.

Zappa, G. (2019). Regional climate impacts of future changes in the mid–latitude atmospheric circulation: a storyline view. *Current Climate Change Reports*, *5*(4), 358–371.

Zappa, G., Ceppi, P., & Shepherd, T. G. (2020). Time-evolving sea-surface warming patterns modulate the climate change response of subtropical precipitation over land. *Proceedings of the National Academy of Sciences*, *117*(9), 4539–4545.

Zappa, G., Hoskins, B. J., & Shepherd, T. G. (2015). The dependence of wintertime mediterranean precipitation on the atmospheric circulation response to climate change. *Environmental Research Letters*, *10*(10), 104012.

Zappa, G., & Shepherd, T. G. (2017). Storylines of atmospheric circulation change for european regional climate impact assessment. *Journal of Climate*, *30*(16), 6561–6577.